Cancer Science
Japanese Cancer Association JCA
Open Access

Cycloamylose-nanogel drug delivery system-mediated intratumor silencing of the vascular endothelial growth factor regulates neovascularization in tumor microenvironment

Hidetaka Fujii,[1,2] Masaharu Shin-Ya,[1] Shigeo Takeda,[3] Yoshihide Hashimoto,[3,4] Sada-atsu Mukai,[3,4] Shin-ichi Sawada,[3,4] Tetsuya Adachi,[1,5] Kazunari Akiyoshi,[3,4] Tsuneharu Miki[2] and Osam Mazda[1]

[1]Department of Immunology, Kyoto Prefectural University of Medicine, Kyoto; [2]Department of Urology, Kyoto Prefectural University of Medicine, Kyoto; [3]Department of Polymer Chemistry, Graduate School of Engineering, Kyoto University, Kyoto, Japan; [4]ERATO, Japan Science and Technology Agency, Tokyo, Japan; [5]Department of Dental Medicine, Kyoto Prefectural University of Medicine, Kyoto, Japan

Key words

Drug delivery system, nanogel, renal cell carcinoma, RNA interference, vascularendothelial growth factor

Correspondence

Osam Mazda, Department of Immunology, Kyoto Prefectural University of Medicine, Kamikyo, Kyoto 602-8566, Japan.
Tel: +81-75-251-5330; Fax: +81-75-251-5331;
E-mail: mazda@koto.kpu-m.ac.jp
Kazunari Akiyoshi, Department of Polymer Chemistry, Graduate School of Engineering, Kyoto University, Nishikyo, Kyoto 615-8510, Japan.
Tel: +81-75-383-2589; Fax: +81-75-383-2590;
E-mail: akiyoshi@bio.polym.kyoto-u.ac.jp

Funding information

Japanese Ministry of Education, Culture, Sports, Science and Technology (No. 22114009 and 26861741).

Received May 30, 2014; Revised September 17, 2014; Accepted September 28, 2014

Cancer Sci **105** (2014) 1616–1625

doi: 10.1111/cas.12547

RNAi enables potent and specific gene silencing, potentially offering useful means for treatment of cancers. However, safe and efficient drug delivery systems (DDS) that are appropriate for intra-tumor delivery of siRNA or shRNA have rarely been established, hindering clinical application of RNAi technology to cancer therapy. We have devised hydrogel polymer nanoparticles, or nanogel, and shown its validity as a novel DDS for various molecules. Here we examined the potential of self-assembled nanogel of cholesterol-bearing cycloamylose with spermine group (CH-CA-Spe) to deliver vascular endothelial growth factor (VEGF)-specific short interfering RNA (siVEGF) into tumor cells. The siVEGF/nanogel complex was engulfed by renal cell carcinoma (RCC) cells through the endocytotic pathway, resulting in efficient knockdown of VEGF. Intra-tumor injections of the complex significantly suppressed neovascularization and growth of RCC in mice. The treatment also inhibited induction of myeloid-derived suppressor cells, while it decreased interleukin-17A production. Therefore, the CH-CA-Spe nanogel may be a feasible DDS for intra-tumor delivery of therapeutic siRNA. The results also suggest that local suppression of VEGF may have a positive impact on systemic immune responses against malignancies.

RNAi may provide promising therapeutic intervention against malignancies due to its potential for specific and powerful gene silencing.[1,2] Although various drug delivery system (DDS) carriers have been developed, clinical application of RNAi has rarely been achieved.[3] To this end, safe and efficient DDS for *in vivo* transfer of siRNA or shRNA is required.[4]

The self-assembled nanogel of hydrophobically modified polysaccharides has the following characteristics.[5,6] First, a range of nanogels with different particle sizes, stability and surface modifications can be synthesized, so that a nanogel that can stably incorporate nucleic acids in the nano network may be developed. Second, it is possible to control the release of self-assembled nanogels through the formation of nanogel-integrated macrogel when they are injected subcutaneously or nasally. Third, the positively charged complex will adhere to the cell membrane, whose surface is negatively charged, allowing cellular uptake of siRNA.

Among the various types of nanogel that we investigated, CH-CA-Spe nanogel was used as a new siRNA carrier. CH-CA-Spe formed polymer nanoparticles in 3-D networks, composed of physical cross-linking of polymer chains (Fig. 1a, b).[7,8] Cycloamylose (CA), which is produced by an enzymatic reaction between linear amylose and disproportionating enzymes, is a unique cyclic α-1,4-glucose polymer consisting of more than 100 glucose units.[9] CA can form inclusion complexes with a variety of hydrophobic drugs.[10] Destabilization of the endosomal membrane is essential to increase the transfection efficiency of non-viral nucleic acid delivery systems. Cycloamylose with spermine group acts as an effective plasmid DNA delivery carrier because CA can interact with endosomal membrane components, such as phospholipids or cholesterol, by forming a supramolecular complex, causing membrane instability.[7] Although CA has high potential as a new polysaccharide-based biomaterial, its biomedical application has thus far been limited.

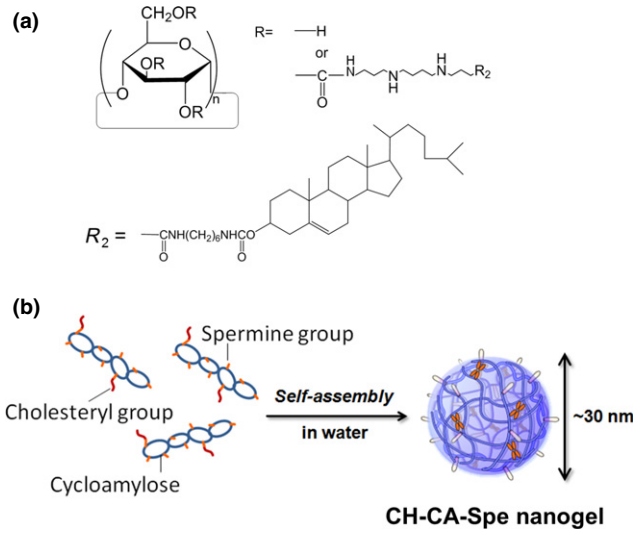

Fig. 1. Structure of CH-CA-Spe nanogel. Schemes of chemical structure (a) and self-assembly (b) of CH-CA-Spe nanogel are shown.

In the present study, we propose the application of cycloamylose-nanogel as a DDS for siRNA-based cancer therapy. We targeted the VEGF gene that could play a key role in tumor-induced neo-angiogenesis. Moreover, we also analyzed whether the local suppression of VEGF in tumors could affect systemic immunity in mice.

Materials and Methods

Synthesis of CH-CA-Spe nanogel. CH-CA-Spe nanogel (Fig. 1a) was synthesized as described previously.[8] Briefly, cationic spermine groups were attached to CA (Mn = 1.9 × 10^4 g/mol, Mw/Mn = 1.08, DP ≈ 100, gifted from Ezaki Glico, Osaka, Japan) by conventional 1,1′-carbonyldiimidazole (CDI) activation. Spermine derivatives showed superior activity for the transfection of siRNA. The spermine-bearing CA (CA-Spe) thus obtained was reacted with cholesteryl *N*-(6-isocyanatohexyl)carbamate. The degrees of substitution of cationic groups and cholesterol in the CA derivative (CH-CA-Spe) were 25 and 3.1, respectively, in 100 glucose units of CA (Fig. 1a).

siRNA and siRNA/CH-CA-Spe nanogel complex. The three siRNA duplexes targeting murine VEGF-A, that are, MSS212359 (siVEGF#59), MSS278683 (siVEGF#83) and MSS278684 (siVEGF#84), were purchased from Invitrogen (Carlsbad, CA, USA). Among them, the MSS278684 (siVEGF#84) showed the highest silencing efficiency (Fig. S1a,b), so this VEGF-specific short interfering RNA (siVEGF) was used as the representative siVEGF in the present study. Control non-silencing siRNA (siCont) (MISSION siRNA Universal Negative Control), FITC-labeled non-silencing siRNA and human VEGF-A specific siRNA[11] were purchased from Sigma-Aldrich (St. Louis, MO, USA). 6-Carboxyfluorescein (FAM)-labeled negative control siRNA was purchased from Life Technologies (Waltham, MD, USA). To form siRNA/CH-CA-Spe nanogel complex, 10 μL each of siRNA (50 μM) and CH-CA-Spe nanogel (21.8 mg/mL) solutions were swiftly mixed, and incubated for 30 min at 25°C, so that the cation/phosphate (C/P) ratio of the resultant complex equaled 10 (C/P = 10). In some experiments different volumes of CH-CA-Spe nanogel were added to the 10 μL of siRNA solution in such a manner that the resultant complex contained 0.8 μg siRNA/10 μL and C/P ratios were 5, 10 or 15. The mixture was diluted to 1:5 with culture medium before transfection.

siRNA transfection *in vitro*. A murine RCC cell line, Renca, and human RCC cell lines, ACHN and 786-O, were resuspended in RPMI1640 medium supplemented with 100 U/mL penicillin, 100 μg/mL streptomycin and 10% FBS and seeded into 24-well tissue culture plates at a density of 5 × 10^4 cells per well at 37°C in 5% CO_2/95% humidified air (standard conditions). The next day, siRNA/nanogel complex was added into culture (5, 10 or 15 μL/well), followed by culturing under standard conditions until analysis. In some experiments, siRNA was transfected by cationic liposome (Lipofectamine RNAiMAX Reagent; Invitrogen) according to the manufacturer's instructions.

Real-time RT-PCR. Total RNA was reverse-transcribed and subjected to quantitative real-time PCR using a 7300 Real-time PCR System (Applied Biosystem, Carlsbad, CA, USA) using primers and probes shown in Table S1. mRNA levels were quantified by RQ software (Applied Biosystems) and standardized relative to the level of the 18S ribosomal RNA or human GAPDH mRNA.

ELISA. Concentrations of VEGF in culture supernatants were measured by ELISA using a mouse VEGF Assay kit (Immuno Biological Laboratories, Tokyo, Japan).

***In vivo* transfection into Renca tumor.** Animal experiments were carried out in accordance with the institutional guidelines of the Kyoto Prefectural University of Medicine. To establish tumor-bearing mice, 5 × 10^5 Renca cells were inoculated s.c. into the right flank of female 7–9 week-old BALB/c mice (Shimizu Laboratory Supplies, Kyoto, Japan). Fourteen days later, tumors developed to an average volume of 50 mm^3 (day 0), into which 50 μL of siRNA/nanogel complex composed of 442.5 μg of CH-CA-Spe and 20 μg of siRNA was injected via a 30-gauge needle on days 0, 4, 8, 12 and 16. The diameters of subcutaneous tumors were measured using a digital caliper, and tumor volume was calculated as $(A^2 \times B)/2$, where A and B are the longest diameter and shortest width of the tumor, respectively. The mice were killed 20 days later.

Flowcytometry. To analyze myeloid-derived suppressor cells (MDSC) populations, spleen cells were stained with allophycocyanin (APC)-conjugated CD11b, FITC-conjugated anti-Gr-1 (Miltenyi Biotec, Bergisch Gladbach, Germany) antibodies. To analyze Tregs, the spleen cells were stimulated with 2 μg/mL of Mouse T-Activator CD3/CD28 antibodies (Life technologies), 10 ng/mL recombinant transforming growth factor (rTGF)-β1 (Pepurotech, Rock Hill, SC, USA) and 200 IU/mL rIL-2 (Pepurotech) for 48 h, followed by staining with PE-conjugated CD4 (eBioscience, San Diego, CA, USA), APC-conjugated CD25 (BD Biosciences, San Jose, CA, USA) and FITC-conjugated anti-Foxp3 (Mouse Th17/TregPhenotyping Kit; BD Biosciences) antibodies. Cells were analyzed by FACS Canto II (BD Biosciences) using the FlowJo software (Tree Star, San Carlos, CA, USA).

Statistical analysis. Data were expressed as means ± SD. The statistical analyses were performed using Student's *t*-test. $P < 0.05$ was considered statistically significant.

Results

Effective delivery of vascular endothelial growth factor-specific short interfering into tumor cells by means of CH-CA-Spe nanogel. CH-CA-Spe nanogel was mixed at various C/P ratios with a siVEGF duplex that had been selected as the most effective among the three different siVEGF duplexes tested (Fig. S1a,b). After incubation under various conditions, the mixtures were

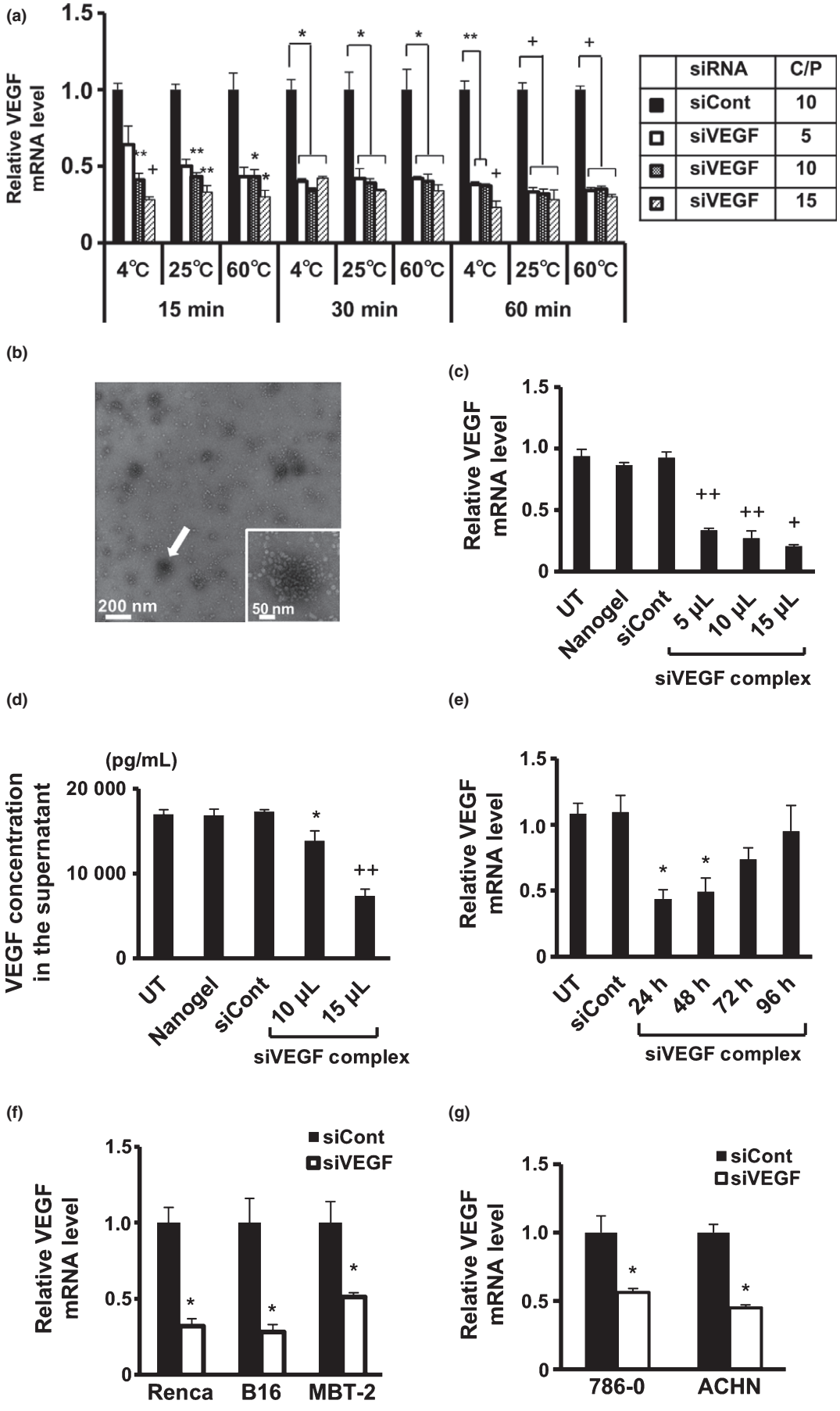

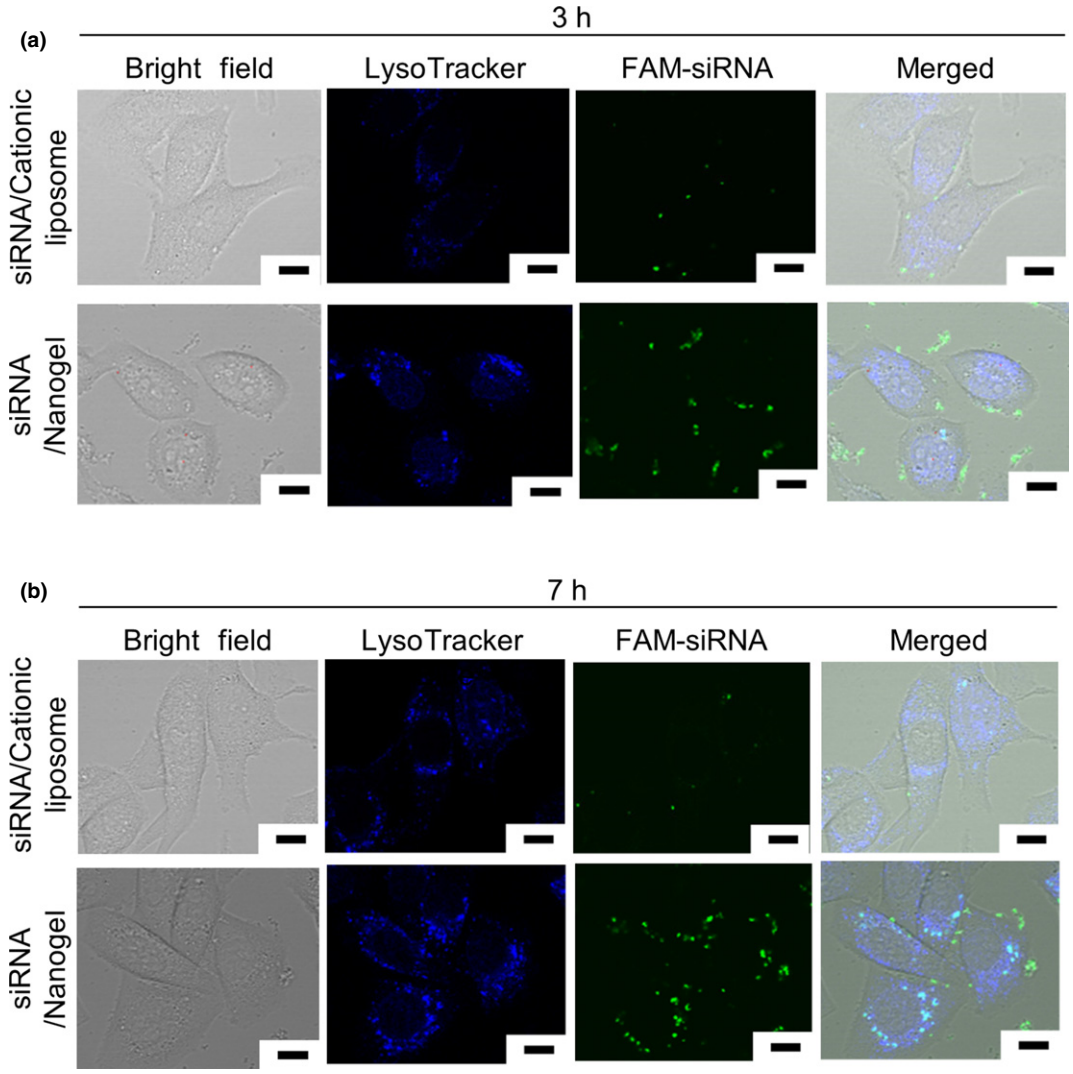

Fig. 3. 6-carboxyfluorescein (FAM)-labeled siRNA (FAM-siRNA)/CH-CA-Spe nanogel complex was endocytosed by tumor cells. Renca cells were transfected with 6-carboxyfluorescein (FAM)-labeled siRNA by means of CH-CA-Spe nanogel or cationic liposome. Three (a) and seven (b) hours later, lysosomes were stained with LysoTracker Blue DND-22 (Life Technologies) and visualized by confocal laser scanning microscopy. Scale bars represent 10 μm.

added to the culture of Renca cells. Efficient silencing of VEGF mRNA was obtained when the mixture was prepared at the C/P ratios of 10 and 15, regardless of the temperatures and incubation periods tested (Fig. 2a). Colloidal siRNAs /nanogel particles were formed under these conditions (Fig. 2b). The siVEGF/nanogel complex suppressed VEGF expression in Renca cells in a dose-dependent manner (Fig. 2c,d), and the silencing effect persisted for 2 days (Fig. 2e). A similar effect was obtained using B16 and MBT-2 (murine melanoma and bladder cancer cell lines, respectively) as well as 786-O and ACHN (human RCC cell lines) (Fig. 2f,g), suggesting effective nanogel-mediated delivery of siRNA into various tumor cells. The siVEGF/nanogel complex did not show any significant toxicity toward the cells (Fig. S1c).

siRNA/nanogel complex was engulfed by tumor cells via lysosomal pathway. Intracellular transport of the siRNA/nanogel complex was analyzed by confocal laser scanning microscopy.

Fig. 2. Vascular endothelial growth factor (VEGF)-specific short interfering RNA (siVEGF)/CH-CA-Spe nanogel complex suppressed VEGF expression *in vitro*. (a) siVEGF/nanogel complex was prepared under the indicated conditions and added to Renca cell culture (0.8 μg of siRNA/10 μL /well). Twenty-four hours later, VEGF mRNA levels were evaluated by real-time RT-PCR analysis. (b) Transmission electron micrograph image of siVEGF/CH-CA-Spe nanogel complex formed at the cation/phosphate (C/P) ratio of 40 at 25°C for 30 min (concentration: 0.8 μg of siRNA/10 μL). The white small dots represent nanogel particles, and the white arrow indicates colloidal siRNA/nanogel complex with a diameter of 50–100 nm. (c and d) Renca cells were transfected with siVEGF/nanogel complex (0.8 μg of siRNA/10 μL) at different doses, while control groups were transfected with control non-silencing siRNA (siCont)/nanogel (0.8 μg of siRNA/10 μL) or left untransfected (UT). Twenty-four hours later, real-time RT-PCR (c) and ELISA (d) analyses were performed. (e) VEGF mRNA was measured by real-time RT PCR at the indicated period after transfection with siVEGF/nanogel complex (0.8 μg of siRNA/10 μL/well). (f and g) The indicated cells were transfected with siVEGF/nanogel complex (0.8 μg of siRNA/10 μL) at doses of 15 (f) and 10 (g) μL/well, and real-time RT-PCR analysis was performed 24 h later. Data represent the means ± SD ($n = 3$). *$P < 0.05$ versus siCont; **$P < 0.01$ versus siCont; +$P < 0.001$ versus siCont; ++$P < 0.005$ versus siCont.

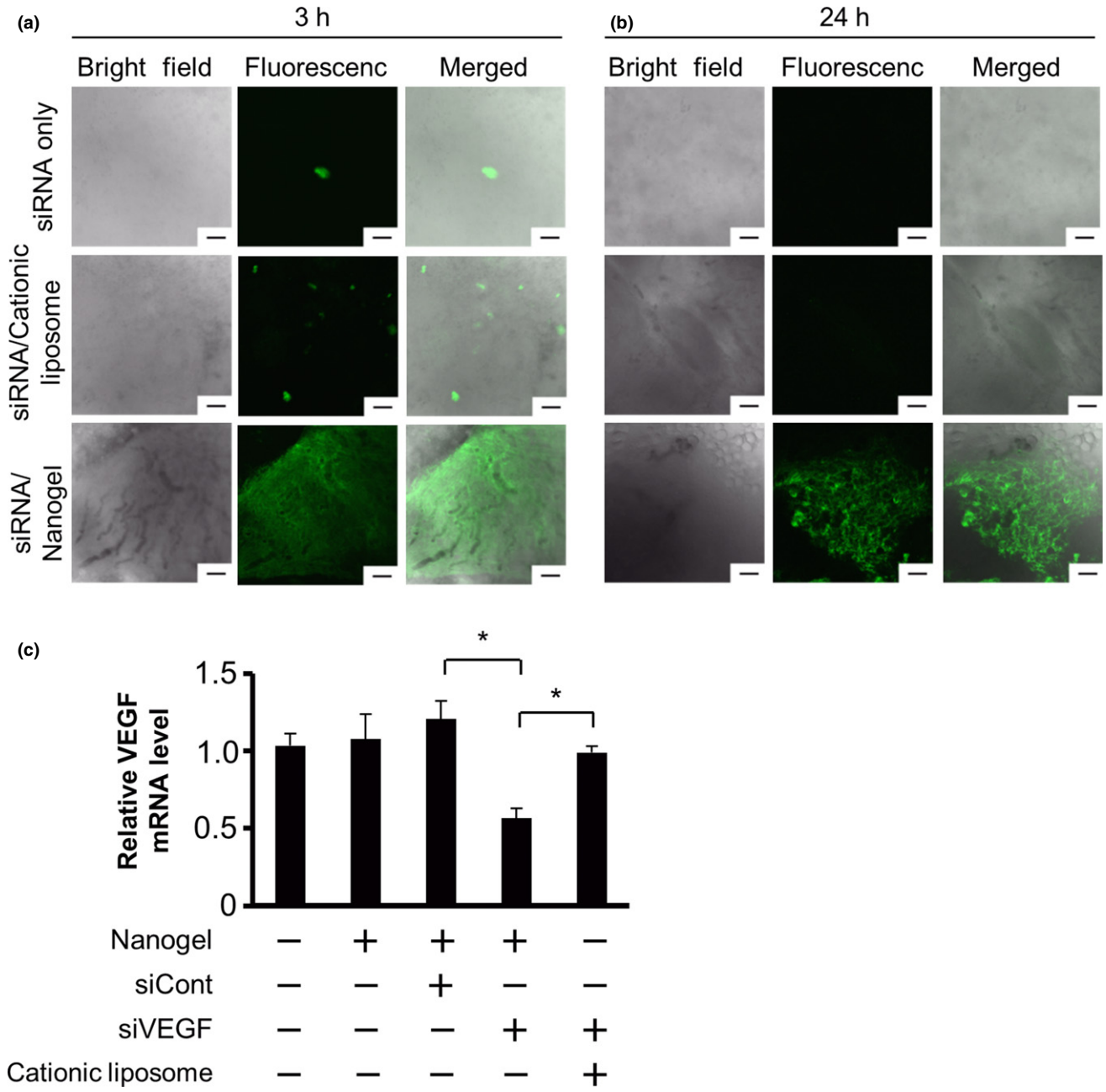

Fig. 4. CH-CA-Spe nanogel enabled effective intratumor siRNA delivery and silencing of vascular endothelial growth factor (VEGF). Tumor-bearing mice were injected with FITC-siRNA alone, FITC-siRNA/cationic liposome complex and FITC-siRNA/nanogel complex into preestablished subcutaneous renal cell carcinoma (RCC) tumors (20 μg of siRNA/50 μL/tumor). Three (a) and twenty-four (b) hours later, the tumor tissue was observed under confocal laser scanning microscopy. Representative bright field (left), fluorescent (middle) and merged (right) images are shown. Scale bar, 100 μm. (c) Tumor-bearing mice were given an intratumoral injection with siRNA/nanogel complex (20 μg of siRNA/50 μL/tumor) or drug delivery system alone, as indicated. Twenty-four hours later, VEGF mRNA levels were measured by real-time RT-PCR. Data represent the means ± SD (n = 5–7).*P < 0.05 versus control non-silencing siRNA (siCont) or cationic liposome group.

FAM (green fluorescence)-labeled siRNA was incorporated into CH-CA-Spe nanogel, and added to Renca cells. Lysosome was stained with LysoTracker (fluorescent blue) and observed at different time points. As shown in Figure 3a, FAM-siRNA was present on the surface of the cells 3 h after addition of the complex. Seven hours after the transfection, the FAM-siRNA

Fig. 5. Vascular endothelial growth factor (VEGF)-specific short interfering RNA (siVEGF) CH-CA-Spe nanogel complex suppressed growth of Renca tumors *in vivo*. Tumor-bearing mice (n = 6) were given intratumor injections with 50 μL of nanogel alone or the indicated siRNA/nanogel complex on days 0, 4, 8, 12 and 16. A group of mice were left untransfected (UT). (a) Growth curves of the tumors are shown. (b–g) Mice were killed on day 20. Representative macroscopic images (b) and weight (n = 6) (c) of the tumors are shown. VEGF mRNA levels in the tumors (n = at least 4/group) (d) and VEGF levels in the sera (n = 5) (e) were measured by real-time RT-PCR and ELISA, respectively. Cryosections of tumors were immunostained with CD31 antibody (f) and microvessel density was calculated (n = 4) (g). Data represent the means ± SD. *P < 0.05 versus control non-silencing siRNA (siCont); **P < 0.01 versus siCont; +P < 0.001 versus siCont. Original magnification in (f) was ×200.

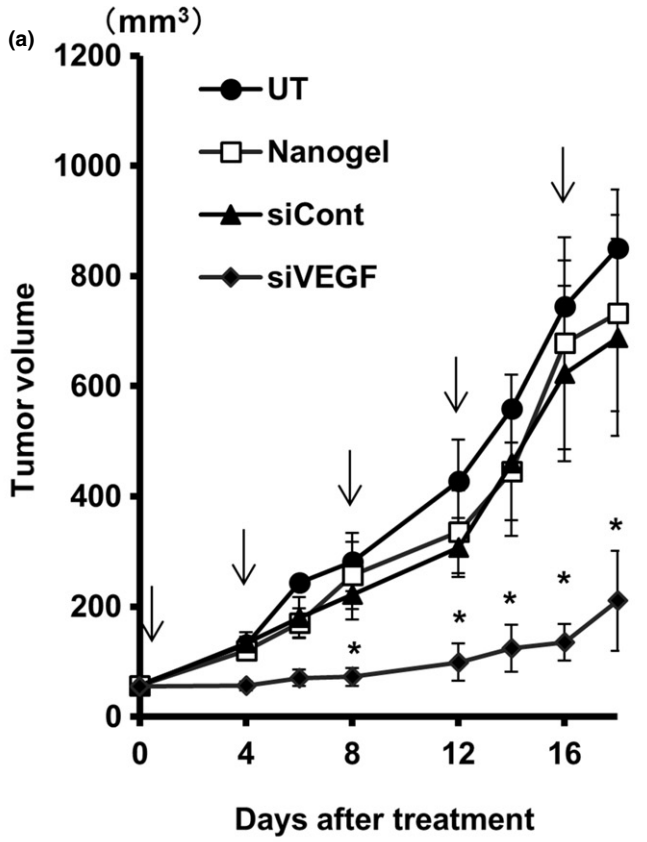

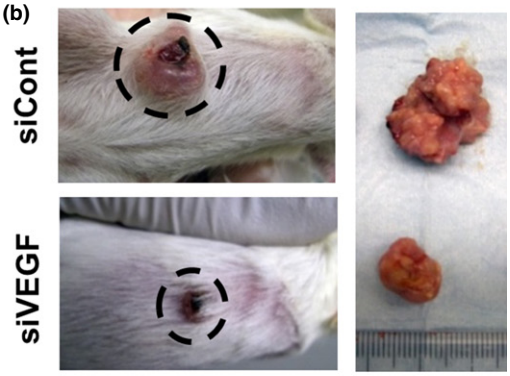

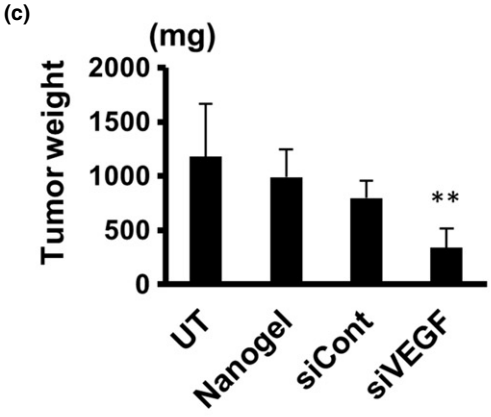

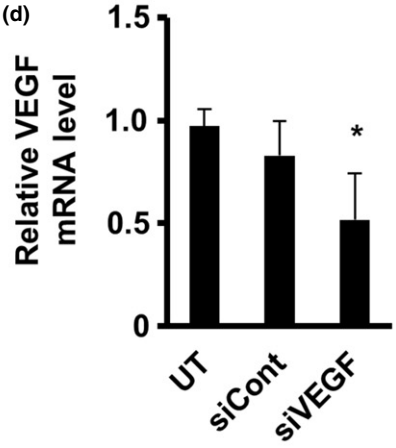

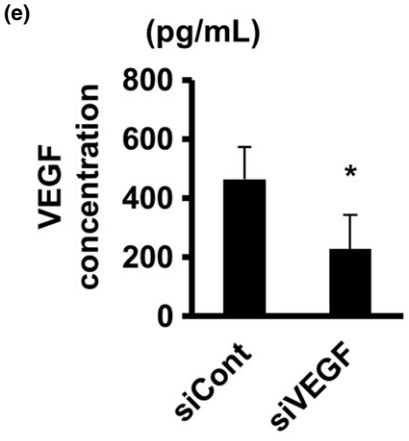

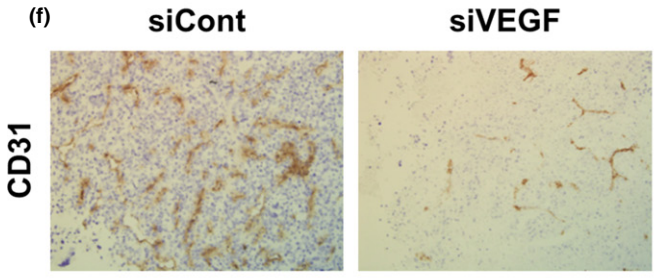

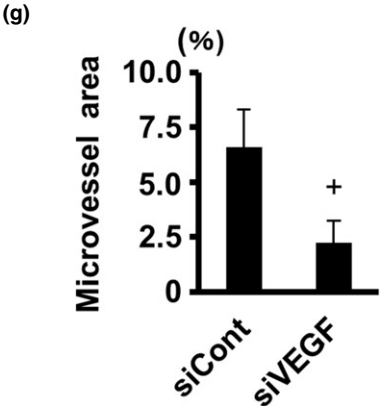

was localized at the lysosomal compartment as demonstrated by a cyan fluorescence in the merged image (Fig. 3b).

Effective intra-tumor delivery of siRNA by CH-CA-Spe nanogel. Successively, to assess *in vivo* localization and stability of the siRNA that was delivered into tumors by CH-CA-Spe nanogel, we injected FITC-labeled siRNA alone or in combination with cationic liposome or nanogel into pre-established RCC tumors in mice. In the tumors that received FITC-siRNA alone, we could detect an extremely sparse distribution of signals, while a sparse signal was scattered in the tumor tissues of the FITC-siRNA/cationic liposome complex. In sharp contrast, we could confirm greater fluorescence signals widely distributed in the FITC-siRNA/nanogel-injected tumors (Fig. 4a). Twenty-four hours after the injection, the FITC signal was clearly observed only in this group (Fig. 4b). Therefore, it appears that siRNA delivered by means of the CH-CA-Spe nanogelis stably maintained in tumor tissue.

Next, to evaluate silencing activity *in vivo*, we injected siVEGF/nanogel complex into the RCC tumors in mice. Twenty-four hours later, real-time RT-PCR demonstrated that the VEGF mRNA in siVEGF/nanogel-injected tumors was suppressed by 42.2% compared with that in an untransfected control. In contrast, a control complex containing the same amount of siRNA but not nanogel did not silence the expression of VEGF to a significant degree (Fig. 4c).

Inhibition of tumor growth and neovascularisation by vascular endothelial growth factor-specific short interfering/CH-CA-Spe nanogel complex *in vivo*. To assess whether siVEGF/nanogel suppresses tumor growth *in vivo*, mice that had been transplanted with Renca cells were given repetitive administrations of the complex, and tumor growth was monitored. As shown in Figure 5a, the siVEGF/nanogel complex significantly suppressed tumor growth, while tumors treated with control complex or nanogel alone showed comparable growth rates as non-treated tumors. These observations were confirmed by macroscopic (Fig. 5b) and gravimetrical quantification (Fig. 5c). Real-time RT-PCR revealed that VEGF mRNA was significantly reduced in the tumors treated with siVEGF/nanogel (Fig. 5d). Serum levels of VEGF were also measured by ELISA, demonstrating a significant decrease in VEGF concentration in the sera of the siVEGF/nanogel-treated animals (Fig. 5e).

We confirmed the anti-tumor effect of siVEGF/CH-CA Spe nanogel complex using two different siVEGF duplexes, while some mice were given intra-tumor administration of siVEGF without nanogel. Both siVEGF duplexes significantly suppressed tumor growth (Fig. S2a) and reduced VEGF mRNA expression in the tumor (Fig. S2b), if they had been coupled with CH-CA Spe nanogel. Such effects were not obtained by siVEGF alone, strongly suggesting the validity of CH-CA Spe nanogel as a DDS for siRNA transfer into tumor.

To estimate whether the siVEGF knockdown therapy had an effect on neovascularization in Renca tumor tissues, vasculature in the tumor sections were immunostained with CD31 antibody and microvessel density were analyzed. The blood vessel formation in the tumors was drastically diminished in siVEGF/nanogel-treated mice compared with that in the control group (Fig. 5f). Quantification of the CD31 staining area revealed that the vasculature occupied a significantly smaller area in siVEGF/nanogel-treated tumors than in siCont/nanogel-treated tumors (Fig. 5g). The siVEGF/nanogel treatment did not affect mice body weight. These results suggested that the CH-CA-Spe nanogel enabled *in vivo* delivery of siRNA, and the RNAi-based therapeutic targeting of VEGF effectively suppressed RCC growth in this subcutaneous tumor-bearing mouse model.

Intratumor administration with vascular endothelial growth factor-specific short interfering/CH-CA-Spe nanogel reduced myeloid-derived suppressor cells and interleukin-17A producing cells in the spleen. We assessed the potential influence of intratumor VEGF silencing on systemic immunity. To this end, we estimated the accumulation of MDSC in spleens of the nanogel-treated mice. The percentage of splenic $CD11b^+Gr1^+$MDSC significantly decreased in the siVEGF/nanogel-treated mice compared with that in siCont/nanogel-treated mice (Fig. 6a). MDSC activity was visualized by diaminofluorescein-2 (DAF-2) assay, and the results revealed that MDSC with high nitric oxide (NO) producing activity[12] were considerably abundant in the control group but not in the siVEGF/nanogel-treated group (Fig. 6b). In addition, we stained the tumor sections with CD11b and anti-Gr-1 antibodies, and found fewer stained cells present in the siVEGF/nanogel treated-tumors than in the control tumors (Fig. 6c). These results strongly suggest that MDSC in spleens and tumors were reduced after the VEGF-silencing using the nanogel.

Next, we analyzed the possible influence of intra-tumor VEGF silencing on splenic regulatory T (Treg) cells. Mouse spleen cells were cultured under Treg-inducing conditions (CD3 and CD28 antibodies, rTGF-β1 and rIL-2). FACS analysis indicated that comparable proportions of $CD4^+CD25^+Foxp3^+$Treg cells were induced from the siVEGF/nanogel-treated mouse spleen cells and from control spleen cells (Fig. S3).

Finally, cytokine production by mitogen-stimulated spleen cells was analyzed by Cytometric Bead Array assay. The results indicated that induction of IL-17A-producing cells was remarkably hampered in spleen cells from mice given intratumor administrations of siVEGF/nanogel (Figs 6d and S4).

Discussion

VEGF is considered to be involved in the process of new vasculature formation, and is recognized as one of the critical players of tumor-induced angiogenesis that is essential for the survival and sustained growth of rapidly proliferating cancer cells.[13–15] In this context, for the inoperable progressive cancers, the molecular target drugs against VEGF have been shown to be efficacious, at least for a short period, in the treatment of inoperable advanced RCC.[16] However, the long-term efficacy of these therapies remains unsatisfactory, and they may cause serious or life-threatening adverse events in some patients.[16]Therefore, it is desirable to develop novel and safe therapeutic procedures for intra-tumor VEGF suppression.

J. Chen *et al.*[17] administered VEGF-specific siRNA by means of hydrophobic poly-(amino acid)-modified polyethylenimine (PEI) into CT26 colorectal cancer transplants in mice, resulting ina 30% decrease in intra-tumor VEGF levels and inhibition of tumor growth by 85%. C.-J. Chen *et al.*[18] incorporated siVEGF in poly-amidoamin with cholesterol moieties, and injected the complex into MCF-7 breast cancer cell xenograftsin mice, resulting in approximately 70% inhibition of tumor growth. Our CH-CA-Spe nanogel enabled successful transfection of siRNA into some human and murine cancer cells *in vitro* (Fig. 2f,g) as well as Renca tumors *in vivo* (Figs 4c and 5d,e), and the growth of Renca tumors was suppressed by 70% (Fig. 5a–c). Compared with previously reported DDS, an important advantage of our physically cross-linked (self-assembled) nanogels is that they are composed of biodegradable components, including cycloamy-

lose that is digested by α-amylase, and spermine and cholesteryl moieties that are also metabolized in the body. This may result in biodegradation *in vivo* of the nanogels after siRNA delivery. Moreover, toxic cross-linkers, catalysts and byproducts are not required in the preparation of the nanogels.[5] The biodegradability and low toxicitymay may be extremely important for clinical application of RNAi therapeutics in the future.

It is noteworthy that the self-assembled nanogels have high retentivity in tumor tissue (Fig. 4b). The high retentivity *in vivo* of the nanogels was also demonstrated in nasal mucosa in our previous study.[19] Because the nanogels have 80–90% water content, the nanogel suspension has a low viscosity and can be easily injected into the tumor. In tumor tissue, however, the water in the solvent permeates the surrounding tissue, while the penetration of nanogel is lower due to its particle size. As nanogel condenses at the injection site, an increase in viscosity and formation of macrogel-like structures by self-assembly of nanogels lead to sustained release of the nanogels from the macrogel (Fig. S5).

Recent reports showed that the therapeutic outcome achieved by VEGF-targeting therapy is much more complicated than previously considered, including modification of immune responses upon tumor progression.[14,20,21] For example, Rosenberg's group demonstrated that inhibition of tumor vasculature with anti-VEGF antibodies facilitated extravasation of adoptively transferred T cells into the tumor tissues and enhanced the clinical efficacy of adoptive cell transfer-based immunotherapy in mice tumor models.[22] We analyzed the influence of intratumor VEGF knockdown on MDSC in the spleen. MDSC are immature myeloid cell populations, characterized by the cell surface expression of Gr-1 and CD11b.[23] They suppress NK and T cells by producing reactive oxygen species (ROS) and inducing Tregs.[24] In tumor-bearing animals and patients, MDSC accumulate in the blood, lymphoid and tumor tissues and are associated with promotion of cancer cell proliferation, angiogenesis and metastasis.[25,26] In the present study, the percentage of MDSC was significantly decreased in the spleens of the siVEGF/nanogel-treated mice (Fig. 6a,b). This is consistent with a previous report that the number of circulating MDSC correlated with serum VEGF levels.[27,28] Therefore, it is conceivable that intra-tumor silencing of VEGF resulted in a decrease in the serum level of cytokine and subsequent inhibition of MDSC, which otherwise contributes to immune escape of the tumors through production of immunosuppressive cytokines, NO and ROS, as well as elevation of arginase-1 activity and induction of Tregs.[27,28]

In the tumor microenvironment, IL-17A-producing T cells are also induced, and they may be involved in the growth and immune escape of the tumors.[29] It has been suggested that

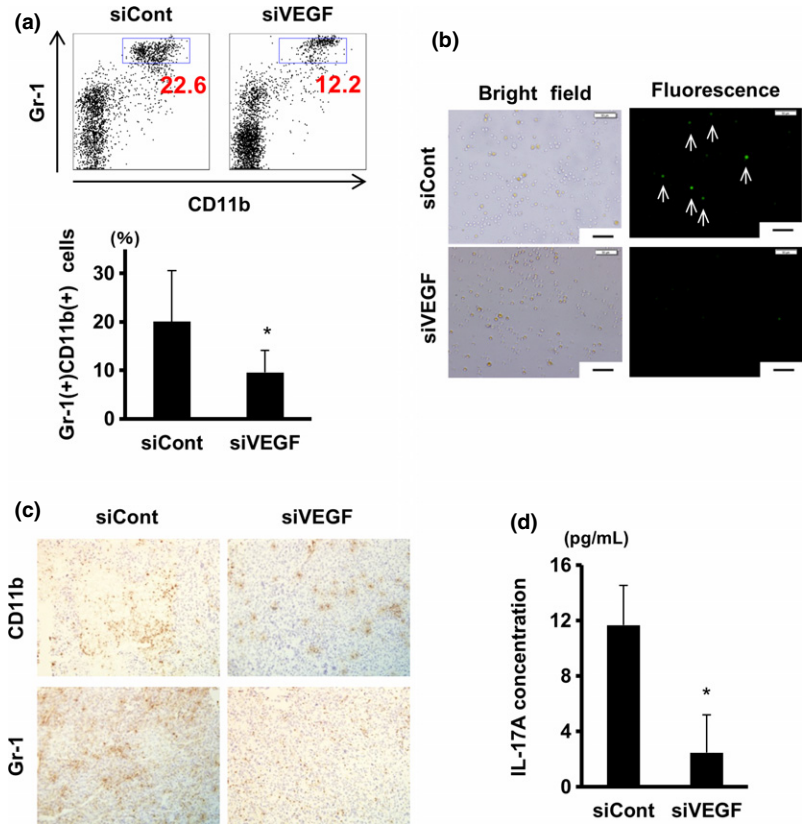

Fig. 6. Vascular endothelial growth factor (VEGF) silencing in tumor significantly suppressed myeloid-derived suppressor cells (MDSC) and interleukin-17A (IL-17A) induction in the spleen. Tumor-bearing mice were given intratumor injections with nanogel alone or siRNA/nanogel complex as in Figure 5. Mice were killed on day 20. (a) Spleen cells were stained with FITC-anti-Gr1 and APC-CD11b antibodies followed by FACS analysis. Numbers in dot plots (upper) indicate proportions of Gr-1$^+$ CD11b$^+$ cells (blue rectangles), while means ± SD (n = at least 7/group) of Gr-1$^+$ CD11b$^+$ populations are plotted (lower). (b) Spleen cells were cultured with interferon (IFN)-γ and LPS, and nitric oxide (NO)-producing cells were visualized by DAF-2 DA. Arrows indicate NO high producer cells. Scale bar, 50 μm. (c) Immunohistochemical staining of the tumor sections with CD11b (upper) and anti-Gr-1 (lower) antibodies. Original magnification was 200×. (d) Spleen cells were cultured with conA, and 24 h later IL-17A concentrations in culture supernatant were measured by the Cytometric Bead Array assay. Data represent the means ± SD (n = 3). *P < 0.05.

the IL-17A-producing T cells may promote tumor vessel formation and proliferation of tumor cells,[29,30] although more detailed mechanisms underlying the linkage between the local VEGF suppression and systemic immunity should be analyzed in future studies.

In conclusion, our siRNA/CH-CA Spe nanogel complex may offer a promising therapeutic procedure characterized by low toxicity to patients, efficient intra-tumor delivery and high stability of siRNA *in vivo*. The present study strongly suggested that local regulation of VEGF may modulate systemic immune responses. More detailed investigation of the mechanism underlying the relation between anti-VEGF treatment and immune modulation might suggest novel therapeutic approaches against malignancies, such as a combination of nano DDS-mediated RNAi therapy and immunotherapy, while CH-CA-Spe nanogel can be also quite useful in analyzing pathophysiology of various diseases, including neoplasms at the molecular level.

Acknowledgments

This work was supported by grants from the Japanese Ministry of Education, Culture, Sports, Science and Technology (22114009).

Disclosure Statement

The authors have no conflict of interest to declare.

References

1 Zamore PD, Tuschl T, Sharp PA, Bartel DP. RNAi: Double-stranded RNA directs theATP-dependent cleavage of mRNAat 21 to 23 nucleotide intervals. *Cell* 2000; **101**: 25–33.
2 Gartel AL, Kandel ES. RNA interference in cancer. *Biomol Eng* 2006; **23**: 17–34.
3 Miele E, Spinelli GP, Di Fabrizio E, Ferretti E, Tomao S, Gulino A. Nanoparticle-based delivery of small interfering RNA: challenges for cancer therapy. *Int J Nanomedicine* 2012; **7**: 3637–57.
4 Ito T, Yoshihara C, Hamada K, Koyama Y. DNA/polyethyleneimine/hyaluronic acid small complex particles and tumor suppression in mice. *Biomaterials* 2010; **31**: 2912–8.
5 Sasaki Y, Akiyoshi K. Nanogel engineering for new nanobiomaterials: From chaperoning engineering to biomedical applications. *Chem Rec* 2010; **10**: 366–76.
6 Kabanov AV, Vinogradov SV. Nanogels as pharmaceutical carriers: Finite networks of infinite capabilities. *Angew Chem Int Ed Engl* 2009; **48**: 5418–29.
7 Toita S, Soma Y, Morimoto N, Akiyoshi K. Cycloamylose-based biomaterial: nanogel of cholesterol-bearing cationic cycloamylose for siRNA delivery. *Chem Lett* 2009; **38**: 1114–5.
8 Toita S, Sawada S, Akiyoshi K. Polysaccharide nanogel gene delivery system with endosome-escaping function: Co-delivery of plasmid DNA and phospholipase A2. *J Control Release* 2011; **155**: 54–9.
9 Saenger W, Jacob J, Gessler K *et al.* Structures of the common cyclodextrins and their larger analogues-beyond the doughnut. *Chem Rev* 1998; **98**: 1787–802.
10 Tomono K, Mugishima A, Suzuki T *et al.* Interaction between cycloamylose and various drugs. *J Incl Phenom Macrocycl Chem* 2002; **44**: 267–70.
11 Takei Y, Kadomatsu K, Yuzawa Y, Matsuo S, Muramatsu T. A small interfering RNA targeting vascular endothelial growth factor as cancer therapeutics. *Cancer Res* 2004; **64**: 3365–70.
12 Nagaraj S, Gabrilovich DI. Tumor escape mechanism governed by myeloid-derived suppressor cells. *Cancer Res* 2008; **68**: 2561–3.
13 Rolf AB, Jay PO, Victor AS *et al.* Selective inhibition of vascular endothelial growth factor (VEGF) receptor 2(KDR/Flk-1) activity by a monoclonal anti-VEGF antibody blocks tumorgrowth in mice. *Cancer Res* 2000; **60**: 5117–24.
14 Verheul HM, Hammers H, van Erp K *et al.* Vascular endothelial growth factor trap blocks tumor growth, metastasis formation, and vascular leakage in an orthotopic murine renal cell cancer model. *Clin Cancer Res* 2007; **13**: 4201–8.
15 Ferrara N, Kerbel RS. Angiogenesis as a therapeutic target. *Nature* 2005; **438**: 967–74.
16 Eisen T, Sternberg CN, Robert C *et al.* Targeted therapies for renal cell carcinoma: Review of adverse event management strategies. *J Natl Cancer Inst* 2012; **104**: 93–113.
17 Chen J, Tian H, Dong X *et al.* Effective tumor treatment by VEGF siRNA complexed with hydrophobic poly(amino acid)-modified polyethylenimine. *Macromol Biosci* 2013; **13**: 1438–46.
18 Chen CJ, Wang JC, Zhao EY *et al.* Self-assembly cationic nanoparticles based on cholesterol-grafted bioreducible poly(amidoamine) for siRNA delivery. *Biomaterials* 2013; **34**: 5303–16.
19 Nochi T, Yuki Y, Takahashi H *et al.* Nanogel antigenic protein-delivery system foradjuvant-free intranasal vaccines. *Nat Mater* 2010; **9**: 572–8.
20 Christina LR, Kristi DL, Jason ET *et al.* Cytokine levels correlate with immune cell infiltrationafter anti-VEGF therapy in preclinical mouse models ofbreast cancer. *PLoS ONE* 2009; **4**: e7669.
21 Shojaei F, Wu X, Malik AK *et al.* Tumor refractoriness to anti-VEGF treatment is mediated by CD11b+Gr1+ myeloid cells. *Nat Biotechnol* 2007; **25**: 911–20.
22 Shrimali RK, Yu Z, Theoret MR, Chinnasamy D, Restifo NP, Rosenberg SA. Antiangiogenic agents can increase lymphocyte infiltration into tumor and enhance the effectiveness of adoptive immunotherapy of cancer. *Cancer Res* 2010; **70**: 6171–80.
23 Tu S, Bhagat G, Cui G *et al.* Overexpression of interleukin-1beta induces gastric inflammation and cancer and mobilizes myeloid-derived suppressor cells in mice. *Cancer Cell* 2008; **14**: 408–19.
24 Gabrilovich DI, Nagaraj S. Myeloid-derived suppressor cells as regulators of the immune system. *Nat Rev Immunol* 2009; **9**: 162–74.
25 Dolcetti L, Marigo I, Mantelli B, Peranzoni E, Zanovello P, Bronte V. Myeloid-derived suppressor cell role in tumor-related inflammation. *Cancer Lett* 2008; **267**: 216–25.
26 Tu SP, Jin H, Shi JD *et al.* Curcumin induces the differentiation of myeloid-derived suppressor cells and inhibits their interaction with cancer cells and related tumor growth. *Cancer Prev Res* 2012; **5**: 205–15.
27 Kusmartsev S, Gabrilovich DI. Role of immature myeloid cells in mechanisms of immune evasion in cancer. *Cancer Immunol Immunother* 2006; **55**: 237–45.
28 Nakamura I, Shibata M, Gonda K *et al.* Serum levels of vascular endothelial growth factor are increased and correlate with malnutrition, immunosuppression involving MDSCs and systemic inflammation in patients with cancer of the digestive system. *Oncollett* 2013; **5**: 1682–6.
29 Satoh T, Tajima M, Wakita D, Kitamura H, Nishimura T. The development of IL-17/IFN-gamma-double producing CTLs from Tc17 cells is driven by epigenetic suppression of socs3 gene promoter. *Eur J Immunol* 2012; **42**: 2329–42.
30 Das RL, Pathangey LB, Tinder TL, Schettini JL, Gruber HE, Mukherjee P. Breast-cancer-associated metastasis is significantly increased in a model of autoimmune arthritis. *Breast Cancer Res* 2009; **11**: R56.

Supporting Information

Additional supporting information may be found in the online version of this article:

Fig. S1. Nanogel successfully delivers vascular endothelial growth factor-specific short interfering RNA (siVEGF) into Renca cells without significantly reducing cell viability.

Fig. S2. Requirement of nanogel for efficient *in vivo* delivery of vascular endothelial growth factor-specific short interfering RNA (siVEGF).

Fig. S3. Cytokine production by mitogen-stimulated spleen cells from the tumor-bearing mice given siVEGF/nanogel treatment.

Fig. S4. Treg cells in spleen were not influenced by siVEGF administration into tumors.

Fig. S5. Schematic representation of release of nanogel from nanogel-integrated macrogel.

Table S1. RT-PCR primer sequences.

Data S1. Materials and Methods.